Current Applied Physics 14 (2014) 407–414

Contents lists available at ScienceDirect

Current Applied Physics

journal homepage: www.elsevier.com/locate/cap

Influence of zirconium doping on structure, microstructure, dielectric and impedance properties of strontium bismuth niobate ceramics

Vinoth Shanmugam [a], R. Sridarane [b], C. Deviannapoorani [a], Raghavendra Kashyap [a], Ramaswamy Murugan [a,*]

[a] Department of Physics, Pondicherry University, Puducherry 605 014, India
[b] Department of Chemistry, Perunthalaivar Kamarajar Institute of Engineering and Technology, Karaikal, Puducherry, India

ARTICLE INFO

Article history:
Received 4 September 2013
Received in revised form
14 December 2013
Accepted 22 December 2013
Available online 4 January 2014

Keywords:
Ceramics
Aurivillius structure
Dielectric
Impedance

ABSTRACT

Efforts have been made in this work to enhance the dielectric properties of $SrBi_2Nb_2O_9$ (SBN) by partial substitution of Zr^{4+} for Nb^{5+}. Systematic investigations on structure, microstructure, dielectric and impedance properties of the $SrBi_2(Nb_{2-(4/5)x}Zr_x)O_9$ [where, $x = 0$, 0.1 and 0.2] ceramic samples were carried out to understand the effect of substitution of Zr^{4+} for Nb^{5+} in $SrBi_2Nb_2O_9$. The X-ray diffraction (XRD) investigations indicated that the lattice volume of $SrBi_2(Nb_{2-(4/5)x}Zr_x)O_9$ with $x = 0.1$ and 0.2 decreases compared to SBN. The SEM investigations revealed an increase in the size of grains and the change on shape of grains to elongated plate shaped structure with the increase of x ($x = 0.1$ and 0.2) in $SrBi_2(Nb_{2-(4/5)x}Zr_x)O_9$. Higher Curie temperature and enhanced peak dielectric constant at the Curie temperature were observed for both the $SrBi_2(Nb_{2-(4/5)x}Zr_x)O_9$ with $x = 0.1$ and 0.2 ceramic samples compared to SBN. Among the investigated compositions the higher Curie temperature and enhanced peak dielectric constant at the Curie temperature was observed for $SrBi_2(Nb_{2-(4/5)x}Zr_x)O_9$ with $x = 0.1$.

1. Introduction

Bismuth layer structured ferroelectrics with Aurivillius type structure received considerable attention in recent times because of their variety of device applications like non-volatile memory, electro-optical switches, and infrared detectors. Aurivillius family materials with general formula $[Bi_2O_2]^{2+}$ $[A_{n-1}B_nO_{3n+1}]^{2-}$ (where the sites A and B can be occupied by different elements) have a complex structure given by $[Bi_2O_2]^{2+}$ sheets intergrowths with perovskite blocks. Among the bismuth layer structured ferroelectrics (BLSF's), $SrBi_2Nb_2O_9$ (SBN) and its solid solutions have attracted much attention for the development of nonvolatile random access memories (NVRAMs) since they offer several advantages like better fatigue properties, low operating voltages and low leakage current.

The influence of substituting effect in BLSF's was widely reported in literature aimed at improvement of the dielectric and ferroelectric properties [1–7]. In particular, partial substitution of V^{5+} with Nb^{5+} in $SrBi_2Nb_2O_9$ found to have significant enhancement in ferroelectric properties [8–13]. Attempt has been also made to enhance the properties of SBN by partials substitution of Ta^{5+} and W^{6+} for Nb^{5+} in $SrBi_2Nb_2O_9$ [6,14]. In the present work systematic investigations on structure, microstructure, dielectric and impedance properties of the $SrBi_2(Nb_{2-(4/5)x}Zr_x)O_9$ [where, $x = 0$, 0.1 and 0.2] ceramic samples were carried out to understand the effect of substitution of Zr^{4+} for Nb^{5+} in $SrBi_2Nb_2O_9$.

2. Experimental

Compounds of the nominal chemical formula $SrBi_2(Nb_{2-(4/5)x}Zr_x)O_9$ [where, $x = 0$, 0.1 and 0.2] were prepared via conventional solid state reaction method using stoichiometric amount of high purity chemicals $SrCO_3$ (Merck, >99%), Bi_2O_3 (3.5 wt% excess Bi_2O_3 to compensate the weight loss of the Bi_2O_3 during the sintering), Nb_2O_5 and ZrO_2. The powders were ball milled using zirconia balls in 2-propanol for about 6 h using a Pulverisette 7, Fritsch, Germany. After the evaporation of solvent, the mixtures were heated at 700 °C in an open alumina crucible for 12 h and then cooled down to room temperature. The resultant powders were ground again for another 6 h using zirconia balls in 2-propanol. After the evaporation of the solvent, the powders were ground and admixed with 2 wt% polyvinyl alcohol as a binder and uniaxially pressed under 250 Mpa into disks of approximately 10 mm in diameter and about 1–2 mm in thickness. The pellets were sintered in air for 12 h at 1150 °C for $SrBi_2(Nb_{2-(4/5)x}Zr_x)O_9$ [where, $x = 0.1$ and 0.2] and 6 h at 1200 °C for $SrBi_2(Nb_{2-(4/5)x}Zr_x)O_9$ [where $x = 0$] sample.

* Corresponding author. Tel.: +91 413 2654782; fax: +91 413 2656988.
E-mail address: moranamurugan@pec.edu (R. Murugan).

1567-1739/$ – see front matter © 2014 Elsevier B.V. All rights reserved.
http://dx.doi.org/10.1016/j.cap.2013.12.020

The phase formation and crystallinity of the calcined samples were characterized by X-ray diffraction (X'Pert PRO PANalytical), using Cu-K_α radiation of wavelength 1.5418 Å in the range of $20^\circ \leq 2\theta \leq 80^\circ$. Confocal micro-Raman spectra have been recorded at room temperature in the range 50–1000 cm^{-1} using a Raman microscope (Renishaw inVia Reflex) with a 50 mW internal Ar ion laser source of wavelength 514 nm. The microstructure of the sintered sample surface was analyzed by scanning electron microscope (SEM) (Hitachi). Impedance measurements were performed on the prepared pellets using Au-electrodes (Au paste cured at 600 °C for 1 h) over the temperature range from room temperature (30 °C) to 700 °C using a Wayne Kerr precision impedance analyzer 6500B series in the frequency range 20 Hz–15 MHz.

3. Results and discussion

3.1. XRD analysis

The measured powder X-ray diffraction (XRD) patterns of $SrBi_2(Nb_{2-(4/5)x}Zr_x)O_9$ [where, $x = 0$, 0.1 and 0.2] along with the JCPDS pattern of SBN (JCPDS file no. 86-1190) are shown in Fig. 1. The X-ray diffraction peaks of $SrBi_2(Nb_{2-(4/5)x}Zr_x)O_9$ with $x = 0$, 0.1 and 0.2 shown in Fig. 1(b), (c) and (d), matches closely in both positions and relative intensities of the diffraction peaks of the reported SBN (JCPDS (card no 86-1190) as shown in Fig. 1(a)). The XRD pattern of $SrBi_2(Nb_{2-(4/5)x}Zr_x)O_9$ with $x = 0.1$ shown as Fig. 1(c) revealed a single phase layered perovskite structure without any secondary phase, indicating that Zr^{4+} is successfully incorporated into the crystal lattice of SBN. However the XRD pattern of $SrBi_2(Nb_{2-(4/5)x}Zr_x)O_9$ with $x = 0.2$ shown as Fig. 1(d) indicated the presence of $Sr_2Bi_2O_5$ as secondary phase along with the major layered perovskite structure. The XRD pattern of $SrBi_2(Nb_{2-(4/5)x}Zr_x)O_9$ with $x = 0.2$ shown as Fig. 1(d) also revealed the diffraction peaks are relatively broadened compared to that of $SrBi_2(Nb_{2-(4/5)x}Zr_x)O_9$ with $x = 0$ and 0.1. The XRD pattern of $SrBi_2(Nb_{2-(4/5)x}Zr_x)O_9$ with $x = 0.1$ and 0.2 could be indexed to an orthorhombic cell. The structural refinement with the dominant diffraction peaks indicated that the lattice parameters of $SrBi_2(Nb_{2-(4/5)x}Zr_x)O_9$ with $x = 0.1$ have slight changes compared to $SrBi_2Nb_2O_9$ as shown in Table 1. However further substitution of Zr^{4+} for Nb^{5+} i.e. $x = 0.2$ in $SrBi_2(Nb_{2-(4/5)x}Zr_x)O_9$ leads to appreciable decrease of the lattice volume. The addition of zirconium improves the densification process as can be seen in Table 1.

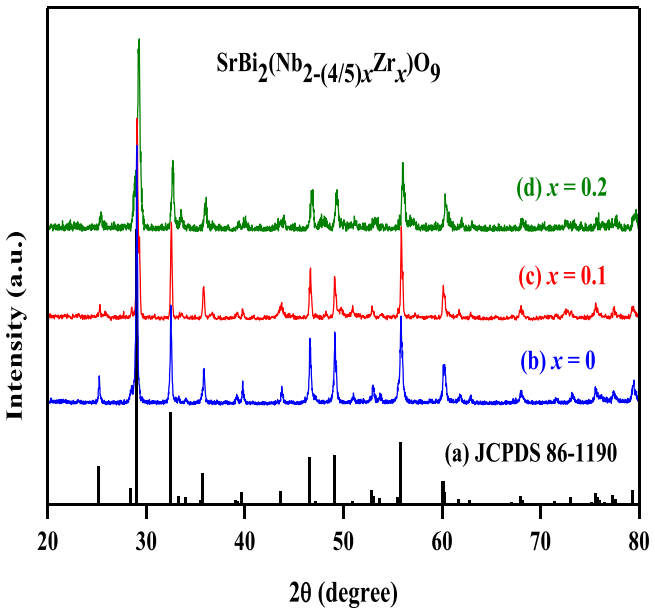

Fig. 1. XRD patterns a) SBN (JCPDS; 86-1190) and $SrBi_2(Nb_{2-(4/5)x}Zr_x)O_9$ with b) $x = 0$, c) $x = 0.1$ and d) $x = 0.2$.

3.2. Raman scattering

The Raman spectra of $SrBi_2(Nb_{2-(4/5)x}Zr_x)O_9$ with $x = 0$, 0.1 and 0.2 samples were measured at room temperature to understand the influence of Zr doping on the vibrational modes of SBN. The Raman spectra measured at room temperature in the spectral range 50–1000 cm^{-1} shown in Fig. 2 revealed that the Raman profiles of $SrBi_2(Nb_{2-(4/5)x}Zr_x)O_9$ with $x = 0.1$ and 0.2 are similar to that of the SBN sample. SBN samples exhibit intense Raman bands at around 66, 202, 577 and 828 cm^{-1} and weak bands at around 170, 300, 446 and 701 cm^{-1}. For the modes above 300 cm^{-1}, the strong band observed at 828 cm^{-1} corresponds to the stretching mode of NbO_6 octahedra and another band observed at 577 cm^{-1} corresponds to a rigid sublattice mode [14–16].

The NbO_6 octahedral stretching mode observed at 828 cm^{-1} for SBN shifted to 837 cm^{-1} for $SrBi_2(Nb_{2-(4/5)x}Zr_x)O_9$ with $x = 0.1$. However further substitution of Zr, i.e. for $SrBi_2(Nb_{2-(4/5)x}Zr_x)O_9$ with $x = 0.2$, the NbO_6 octahedral stretching mode exhibit shift towards lower wave number to 834 cm^{-1}. The NbO_6 octahedral stretching mode appears to be relatively symmetric with Zr substitution. The changes observed in the NbO_6 octahedral stretching mode might be due to the effect of partial substitution of Zr^{4+} for Nb^{5+}. The band observed at 577 cm^{-1} for SBN corresponds to the rigid sublattice mode exhibit red shift to 566 cm^{-1} for $SrBi_2(Nb_{2-(4/5)x}Zr_x)O_9$ with $x = 0.1$ and 569 cm^{-1} for $SrBi_2(Nb_{2-(4/5)x}Zr_x)O_9$ with $x = 0.2$. The mode observed at 66 cm^{-1}, assigned as a 'rigid layer' mode reflecting the Bi^{3+} ions vibration in Bi_2O_2 layers do not exhibit any major shifts with increase in Zr substitution [16]. Similarly the band at 202 cm^{-1} corresponds to the vibrations of A site ions of the pseudo perovskite blocks also do not exhibit any major shift in its position with the Zr substitution in SBN.

3.3. Scanning electron microscope (SEM) analysis

The SEM images of $SrBi_2(Nb_{2-(4/5)x}Zr_x)O_9$ where, $x = 0$, 0.1 and 0.2 are shown in Fig. 3(a)–(c), respectively. The SEM images of all the samples show relatively dense structure, and although small pores were found in the samples. An obvious difference among the images is the grain size which depends on the amount of doped zirconium. The micrograph for SBN shown as Fig. 3(a) indicated that the grains are not well defined. The increase of x in $SrBi_2(Nb_{2-(4/5)x}Zr_x)O_9$ (Fig. 3(b) and (c)) indicated the growth of grain and the change on shape of grains to elongated plate shaped structure. The plate like structure is typical of Aurivillius phase due

Table 1
Lattice parameters, volume and relative density of SBN ($SrBi_2Nb_2O_9$) sintered at 1200 °C, $SrBi_2(Nb_{2-(4/5)x}Zr_x)O_9$ with $x = 0.1$ and $x = 0.2$ samples sintered at 1150 °C.

Composition	Lattice parameters (Å)	Volume $V = abc$ (Å^3)	Relative density (%)
SBN ($SrBi_2Nb_2O_9$)	$a = 5.518$ $b = 5.515$ $c = 25.112$	764.202	94
$SrBi_2Nb_{1.92}Zr_{0.1}O_9$	$a = 5.500$ $b = 5.519$ $c = 25.110$	762.201	95
$SrBi_2Nb_{1.84}Zr_{0.2}O_9$	$a = 5.465$ $b = 5.492$ $c = 25.046$	751.725	98